Electroanatomic Mapping to Support Ablation of Complex Supraventricular Arrhythmias: Does It Matter?

R. De Ponti[1], R. Verlato[2], G. Pelargonio[3], F. Drago[4], A. Fusco[5], J.A. Salerno-Uriarte[1] on behalf of the Investigators of the Project of ElectroAnatomic mapping for Complex arrhythmia Evaluation (PEACE)*

Introduction

Over the last 15 years, experience in catheter ablation of cardiac arrhythmias has greatly increased. This has gone hand in hand with technical improvements and the development of new approaches. Currently, catheter ablation is considered the first-line therapy for arrhythmia exhibiting a 'stereotyped' substrate, such as typical atrial flutter, atrioventricular nodal reentrant tachycardia, and tachycardias mediated by an accessory pathway [1, 2]. For these supraventricular arrhythmias, a high success rate with minimal procedural risks can be obtained by experienced operators in a relatively short-lasting procedure. Conversely, in atypical atrial flutter and, generally, in postsurgical supraventricular arrhythmias, clear definition of the arrhythmia mechanism, extensive mapping, and precise localisation of the target area are required to provide a tailored ablation strategy. Especially in patients with prior surgery for complex congenital heart disease and in the presence of multiple clinical arrhythmias, the ablation procedure may be prolonged, have limited procedural and long-term success, and be associated with a higher risk of complications. In fact, the results of catheter ablation previously reported in this subset of patients and based on conventional mapping were promising but still suboptimal [3–6], considering also that in these patients arrhythmia-related morbidity and mortality are increased compared to the general population with supraventricular arrhythmias.

[1]Department of Cardiovascular Sciences, Ospedale di Circolo e Fondazione Macchi, University of Insubria, Varese; [2]Electrophysiology Laboratory, Ospedale Civile of Camposampiero, Camposampiero (Padua); [3]Institute of Cardiology, Department of Cardiovascular Medicine, Catholic University of the Sacred Heart, Rome; [4]Department of Pediatric Cardiology, Ospedale Bambino Gesù, Rome; [5]Electrophysiology Laboratory, Pederzoli Hospital, Peschiera del Garda (Verona), Italy; *See the Appendix for the list of the other Investigators of the project

Moreover, in some patients, 12-lead ECG can be of very limited help in understanding the arrhythmia mechanism and in orienting the ablation strategy (Fig. 1).

Non-conventional mapping systems have been extensively introduced in the electrophysiology laboratory, especially to assist in diagnosing patients with complex forms of disease and to provide essential information for planning the ablation strategy in patients with a non-stereotyped arrhythmogenic substrate. Recently, single-centre experiences involving a limited number of patients have been reported regarding the use of electroanatomic mapping to support ablation of right or left atypical atrial flutter, and in patients with atrial tachycardias after surgery for congenital and acquired heart disease [7–12]. In these patients, electroanatomic mapping has proved useful to identify the critical area of the tachycardia, especially in double-loop reentry and multiple wavefront collision, providing a road map for ablation of unconventional isthmuses in reentrant arrhythmias [11]. This rationalised approach in patients with complex arrhythmias is expected to lead to optimised short- and long-term results, reducing significantly the procedural difficulties and duration.

To better assess the contribution of electroanatomic mapping to ablative treatment of complex arrhythmias in a larger and multicentre experience, the Project of Electro-Anatomic mapping for Complex Arrhythmia Evaluation (PEACE) was organised in 2003 and coordinated by our University. In this project, roughly a dozen Italian electrophysiology laboratories (see Appendix) with different profiles, but similarly willing to share the experi-

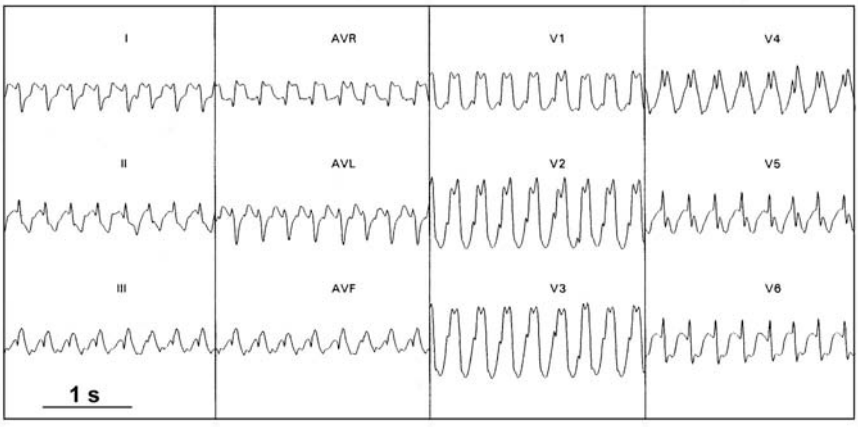

Fig. 1. Clinical atrial tachycardia of the first presented case, showing a cycle length of 290 ms. The wide QRS complex (superimposible to the one on sinus rhythm) does not allow clear visualisation of the surface P wave

ence of approaching complex arrhythmias by electroanatomic mapping, were involved. Over this time period, 41 patients were studied for macro-reentrant or focal atrial arrhythmias with or without prior cardiac surgery or for complex forms (incessant or nonsustained/noninducible) of ventricular tachycardias. In these patients, after their histories were evaluated and pre-procedure diagnostics were obtained, electrophysiologic and extensive electroanatomic evaluations were carried out to plan a rationale for ablation, which was successful in the vast majority of the patients. The following is a presentation of four typical cases involving study patients with postsurgical or postablation focal or macro-reentrant atrial tachycardia/flutter.

Postsurgical Focal Atrial Tachycardia

Focal atrial tachycardia has been reported occasionally as an accompanying arrhythmia in patients with macro-reentrant atrial tachycardia after cardiac surgery [8, 11, 13–17]. In these reports, the overall number of focal atrial tachycardia morphologies was 19 and, with two exception [15, 16], they accounted for less than 10% of the total number of atrial tachycardia morphologies in these series of postsurgical patients. Interestingly, in the majority of the cases (14/19 morphologies), the tachycardia focus was located in the anterolateral wall of the right atrium. In the following, two cases of focal atrial tachycardia in patients previously operated on for congenital heart disease are described.

The first case involves a 43-year-old male patient, who at the age of 15 underwent surgery for tetralogy of Fallot. Ten years later, he began complaining of palpitations, which became more frequent in recurrence and drug refractory. As a result, in 1999, he underwent the first electrophysiology procedure in our institution. Clinical atrial tachycardia at a cycle length of 440 ms was reproducibly inducible and was diagnosed as an intraatrial macro-reentrant tachycardia with the critical isthmus of slow conduction located between the coronary sinus os and the inferior vena cava. Limited radiofrequency energy delivery in that region suppressed the tachycardia, and no other tachycardia was inducible thereafter. Of interest, conventional mapping during sinus rhythm showed two vertical lines of double potentials along the septum and the anterolateral right atrium, likely related to surgical incisions/sutures. Moreover, during programmed atrial stimulation, conduction delay over the anterolateral right atrial wall was observed, with preserved voltage amplitude. The patient remained asymptomatic for the next few years, up to February 2004, when he had palpitation recurrence documented at ECG as the arrhythmia shown in Fig. 1. Since the QRS complex was superimposible on the sinus rhythm, its supraventricular origin was

clear; but the wide QRS complex did not allow analysis of the P-wave morphology. Adenosine injection reproducibly terminated the tachycardia, such that surface ECG did not contribute to orienting the site of origin of the tachycardia. During the same hospital admission, the patient experienced multiple drug-refractory arrhythmia recurrences and therefore underwent electrophysiologic evaluation. At baseline, a nonsustained form of the same tachycardia with 1:1 atrioventricular conduction was present and became sustained with a cycle length of 290 ms during isoprenalin infusion. Electroanatomic mapping was performed during sinus rhythm and atrial tachycardia, with a coronary sinus atriogram as reference signal. Surprisingly, during mapping, a complete absence of electrical activity in a wide right atrial area, which included the anterolateral wall, the cavotricuspid isthmus and a part of the posterior wall, became evident early on (Fig. 2A). A line of double potentials was still recorded along the atrial septum (Fig. 2B). During tachycardia, right atrial activation lasted 148 ms, equal to 51% of the tachycardia cycle length, with a centrifugally spreading activation pattern from the earliest site, located on the crest of the right appendage. Bipolar recording at this site preceded the coronary sinus atriogram by 252 ms and the initial unipolar deflection was completely negative. Even in the absence of identification of the P-wave onset, this finding favoured a focal origin from this site. As also shown in Fig. 2B, later activation of the atrial septum and of the expected site of Bachmann's bundle insertion in the right atrium excluded left-to-right atrial propagation due to a left-sided arrhythmia. In this case, the late diastolic activation of the coronary sinus reflected very delayed inter-atrial propagation, rather than being a consequence of a reentrant left atrial circuit. Analysis of the voltage mapping of the tachycardia (Fig. 2C) and comparison with the map of sinus rhythm (Fig. 2D) evidenced that the tachycardia focus was located in a low-voltage (< 0.6 mV), but still viable area at the border zone of the scar tissue at a distance of 16 mm from the sinus node area. Radiofrequency energy delivery at the earliest activated site by cool-tip catheter (40 Watts) for 45 s produced early and sudden tachycardia termination, with no sign of damage to the sinus node. Two other applications, on sinus rhythm, were then delivered just superiorly and inferiorly to the tachycardia focus. Afterwards, the tachycardia was no longer inducible even at the maximal infusion rate of isoprenalin, and no other arrhythmia was observed. During follow-up on the previously ineffective antiarrhythmic agent (sotalol), the patient has been symptom-free. Interestingly, analysis of the first 15 ms of the propagation map in sinus rhythm and during tachycardia showed a wider activated area in sinus rhythm than on tachycardia, suggesting a more complex anatomic substrate for the sinus node than for the focal atrial tachycardia, which, in this case, required a relatively small amount of energy to be abolished.

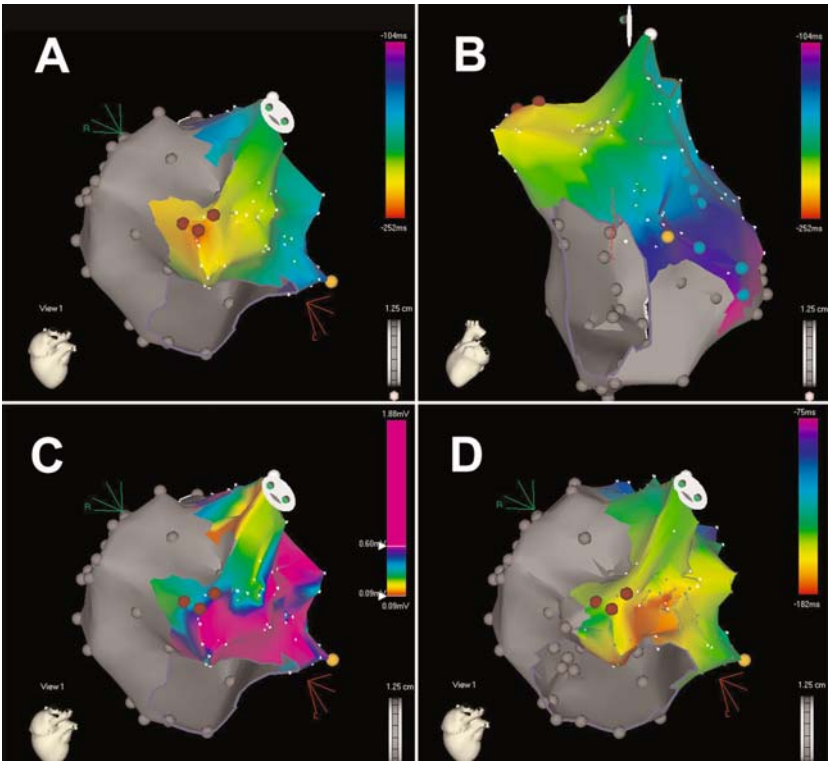

Fig.2. Electroanatomic mapping of the right atrium of the first presented case, during clinical atrial tachycardia (**A–C**) and sinus rhythm (**D**). **A, C, D** Cranial left anterior oblique projection; **B** left lateral view. the extension of the scar tissue (in grey) is well evident in all of the maps. **A, B** Activation mapping in tachycardia, with the earliest activated site (*in red*) in the crest of the right appendage, where ablation is performed (central red dot corresponds to the effective application; the other two dots are bonus applications on sinus rhythm). Moreover, in **B**, the prior atriotomy is evident as a vertical line of double potentials (*blue dots*) along the atrial septum. **C** Bipolar voltage mapping: areas with voltage > 0.60 mV are identified in *purple*. **D** Distance from the ablation site and the extension of the sinus node area (*in red*). See text for further explanation

In this patient, electroanatomic mapping provided very useful data for practical use and for gaining further insight into the patient's arrythmia. In the presence of complex anatomy and in the absence of information provided by P-wave morphology, mapping identified the tachycardia mechanism, excluded involvement of the left atrium, located precisely the arrhythmia focus, and determined its distance from the sinus node to guide ablation successfully and safely. In addition, the progressive and extensive loss of atrial electrical activity, the location of the arrhythmia focus at the border with the scar tissue, together with its different activation pattern as compared to the sinus node posed interesting questions for further study.

The second case involved a 39-year-old female patient with transposition of the great vessels and ventricular septal defect. At the age of 5, she underwent Rastelli's operation at the Mayo Clinic, with external homograft conduit between the right ventricle and the pulmonary artery. Seven years later, she underwent another operation to substitute the conduit. At the age of 35, the patient started developing signs and symptoms of congestive heart failure, with enlargement of both the right atrium and ventricle. Despite optimal medical therapy, she complained of palpitations due to atrial tachycardia and atrial fibrillation. Due to coexistence of life-threatening ventricular arrhythmias, a dual-chamber ICD was implanted. In the months before the procedure, despite therapy with amiodarone and beta-blockers, she developed atrial tachycardia at 400-ms cycle length with 1:1 atrioventricular conduction with periods of incessant-iterative presentation. These were responsible for severe functional limitations and a worsening of heart failure. Similar to the previous case, a wide QRS complex due to right bundle-branch block and 1:1 atrioventricular conduction during tachycardia rendered analysis of the P-wave morphology, especially of its initial deflection, very difficult. During electrophysiologic evaluation, at baseline, under general anaesthesia, the patient was stably on sinus rhythm with right bundle-branch block. Atrioventricular conduction was normal and only antegrade. By S2S3 programmed atrial stimulation during isoprenalin infusion, the clinical atrial tachycardia at a cycle length of 420 ms was reproducibly induced with a 1:1 atrioventricular conduction ratio. The coronary sinus atriogram served as a reference, which allowed initiation of electroanatomic mapping of the right atrium, using a long sheath to support the mapping catheter for the enlarged chamber size. Despite optimal catheter-to-tissue contact, the right atrium lacked atrial electrical activity over a vast area of the anterolateral and posterior walls, which, therefore, were tagged as scar tissue. At the beginning of mapping, the earliest activated site was the medial upper right atrium, where a bipolar signal with an amplitude of 0.61 mV preceded the reference signal by 120 ms. In the same site, a fast negative initial unipolar deflection was recorded. Any attempt to stably change the 1:1 atrioventricular conduction ratio during tachycardia, in order to evaluate P-wave onset and the interval between it and the local bipolar electrogram, was unsuccessful or terminated the tachycardia. Although the local signal and the centrifugally spreading propagation pattern suggested focal atrial tachycardia originating from that site, it was decided to continue mapping, since the geometry of the chamber appeared incomplete in its anterosuperior area. During further mapping, a more anterior site showed an earlier activation (-28 ms compared to the previous site) with a similar unipolar pattern and a bipolar amplitude of 0.87 mV. From there, a channel of low bipolar signals between two areas of scar tissue (Fig. 3A) was identified, leading to the earliest activated site,

which preceded the reference signal by 195 ms (Fig. 3B). In this site, the unipolar deflection could not be evaluated, since it was superimposed on one of the previous ventricular beats. Nonetheless, the atrial origin of the bipolar signal was validated by a single ventricular extrastimulus, which dissociated this signal from the ventricular activity. Based on this evidence and considering the remote position of the sinus node, previously assessed (Fig. 3C), radiofrequency energy at 30 Watts was delivered by cool-tip catheter. This led to early termination and complete suppression of the tachycardia. Subsequently, a second atrial tachycardia with a 500-ms cycle length and negative P wave in the inferior lead was reproducibly induced and then was targeted and successfully ablated as a second focal atrial tachycardia originating in the central part of the cavotricuspid isthmus. During follow-up, the patients had relevant clinical improvement with persistent suppression of the treated forms and only rare nonsustained runs of slow, well-tolerated atrial tachycardia. Interestingly, the analysis of the voltage map of clinical atrial tachycardia (Fig. 3D) showed very low voltage (0.07–0.15 mV) along the channel leading to the tachycardia focus, located also in this case at the border zone between viable and scar tissue, whereas relatively preserved bipolar voltage (> 0.5 mV) was observed at the channel exit. It is not clear why the unipolar signal was negative at sites different and even remote from the site of tachycardia origin. The most likely explanation is that activation of the very low voltage channel was not detected by unipolar recording at the site of exit from the channel. Therefore, the wavefront propagating from this site to the atria was read as negative from the unipolar recording, although remote from the site of origin of the tachycardia.

Thus, also in this case of postsurgical atrial tachycardia, electroanatomic mapping was very useful to search for and localise the tachycardia focus in a very low voltage area at the border with a wide zone of scar tissue in the presence of discordant conventional criteria and of a very distorted atrial anatomy. Similar to the previous case, it could be speculated that the origin of postsurgical focal atrial tachycardia was in the upper right atrium, at the border between the scar and the still viable tissue, which is often not easy to define. Here a progressive process may be responsible for the creation of tachycardia foci, even years after surgery. Due to the unique environment where this form of tachycardia develops, the conventional criteria to identify the tachycardia focus might not be invariably reliable. Moreover, intra-atrial or inter-atrial (as in the previous case) delayed propagation during tachycardia may represent a complexity in clarifying the arrhythmia mechanism (focal vs re-entry). At the same time, it may be responsible for the exception to the rule that during a focal rhythm the atria are activated for a limited part (usually < 50%) of the atrial cycle. Finally, the evidence obtained from voltage mapping of large areas of scar tissue and/or low voltage could give an

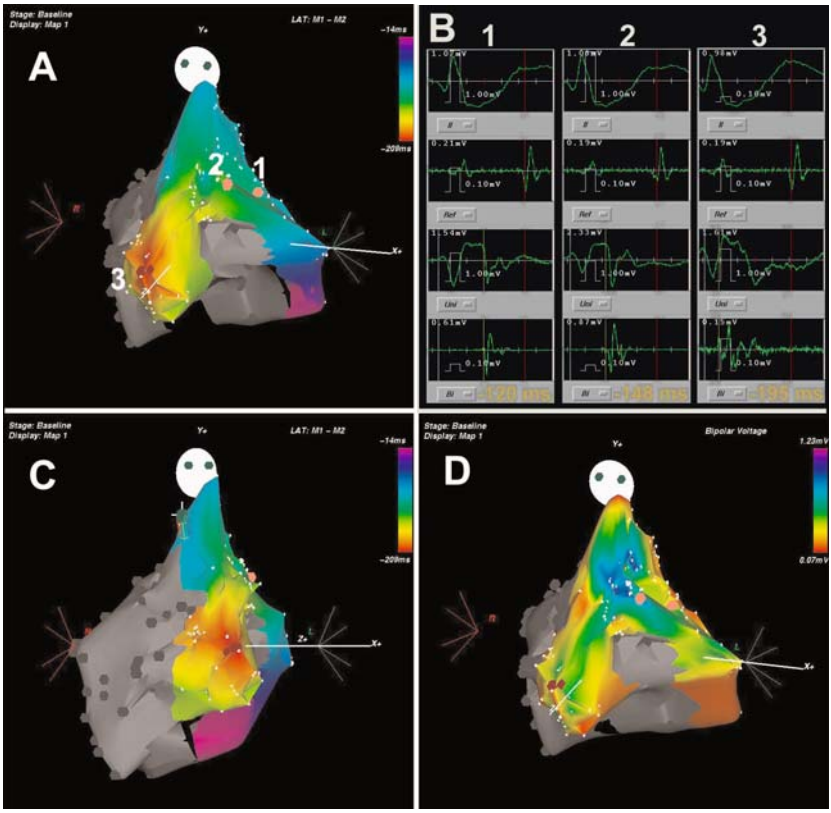

Fig. 3A–D. Electroanatomic mapping of the cranial part of the right atrium during tachycardia in the second presented case. **A, D** Cranial left anterior oblique view; **C** right anterior oblique view. **A** Activation mapping during tachycardia, with the earliest activated site (*in red*) in the antero-ateral area of the superior right atrium, between two areas of scar tissue (*in grey*). The site of successful ablation is marked by *red dots.* **B** From top to bottom, lead II, the reference coronary sinus atriogram (Ref), the unipolar (Uni) and bipolar (Bi) deflections recorded at sites marked as 1, 2 and 3 in the previous panel are shown. Numbers at the bottom express how much earlier the bipolar recording at each site is, as compared to the reference signal. **C** Another view of the activation mapping during tachycardia, which better shows the ablation site and its distance from the sinus node area, where the catheter icon is positioned. **D** Distribution of the bipolar voltage: low voltage (0.07–0.15 mV) is identified by red-to-green colours in the channel between the two scars, where the tachycardia focus is located. See text for further explanation

idea of both the poor haemodynamic contribution of these atria and the prognosis in these patients, especially in term of recurrences and of possible sinus node dysfunction.

Postsurgical/Postablation Macrore-entrant Atrial Tachycardia/Flutter

As already mentioned, surgical atrial incisions may create an isthmus of slow conduction, responsible for re-entrant tachycardia occurring after a variable time interval from surgery. On the other hand, left atrial flutter may occur also after pulmonary vein isolation for atrial fibrillation by percutaneous technique, endangering the long-term success of the procedure [18–21]. Although rare, left atrial flutter may be less tolerated and less responsive to antiarrhythmic drugs than atrial fibrillation. Whether it is due to a focal mechanism [18], a re-entry related to gaps in a linear lesion previously deployed [19], or a combination of the two mechanisms in different patient subsets [20] is still debated. The two cases presented below show how electroanatomic mapping may contribute to an in-depth understanding of the arrhythmogenic substrate in patients with postsurgical/postablation macrore-entrant arrhythmias.

The third case involves a 61-year-old male patient affected by hypertension with only mild dilatation of the left atrium. The patient underwent ablation for typical atrial flutter with complete bidirectional block of the cavotricuspid isthmus conduction at the age of 54. Three years later, he underwent elsewhere electrophysiologically guided pulmonary vein isolation for recurrent atrial fibrillation refractory to multiple antiarrhythmic drugs. During the same hospital stay, he underwent three ablation procedures. Afterwards, he had episodes of palpitation, with ECG documenting atrial tachycardia with a stable cycle length of 260 ms and flat P-wave morphology separated by isoelectric lines in all leads, except for V1, showing a distinct positive P wave. Six months before the procedure, the arrhythmia became persistent and was poorly tolerated. During the procedure, at baseline, the patient exhibited clinical arrhythmia with a variable ratio of atrioventricular conduction. In order to map the expected macrore-entry, the window of interest was set to start in mid-diastole on surface ECG, spanning 95% of the cycle length, as described elsewhere [22]. Electroanatomic mapping in the right atrium did not show a head-meets-tail pattern, entrainment had a return cycle markedly longer than the tachycardia cycle length, and the propagation pattern favoured a left atrial origin. After trans-septal puncture, the left atrium was extensively mapped, which showed an absence of electrical activity in a large area around the oses of the four pulmonary veins and in the posterior left atrium. In the remaining part of the left atrium, between the scar tissue and the mitral ring, the electroanatomic activation map showed electrical activity spanning the entire tachycardia cycle length with a single-loop clockwise re-entry around the mitral annulus (Fig. 4A). Having set the window of interest from mid-diastole to the next mid-diastole, the mid-diastolically activated area was identified as the interface between the red and the

purple area in the activation map. As shown in Fig. 4A, this area was located between the scar tissue around the os of the right pulmonary veins and another small scar at 11 o'clock of the mitral ring. This was possibly a gap in an incomplete linear lesion previously attempted between the mitral ring and the right superior pulmonary vein. In the area identified as critical at the electroanatomic mapping, concealed entrainment with a postpacing interval equalling the tachycardia cycle length was obtained. The bipolar voltage map (Fig. 4B) showed an extensive low voltage (< 0.10 mV) in the critical area, suggesting a relatively easy substrate to ablate. Higher voltage (> 4 mV) was observed in the left atrial appendage. Radiofrequency energy delivery (cool-tip catheter; 35 Watts) in the area identified as critical, where an isolated mid-diastolic potential was recorded, terminated the tachycardia early during the application. Ablation was then continued in the area identified by the interface between the head and the tail of the circuit, in the conducting gap between the two scars, to minimise recurrences. This further ablation produced complete disappearance of electrical activity in this area. Subsequently, no arrhythmia was inducible by aggressive atrial pacing and the patient remained asymptomatic in the follow-up.

This case is paradigmatic of how electroanatomic mapping can reconstruct the re-entrant loop(s), identifying a head-meets-tail pattern and the critical area of mid-diastolic activation. Moreover, the extension and the

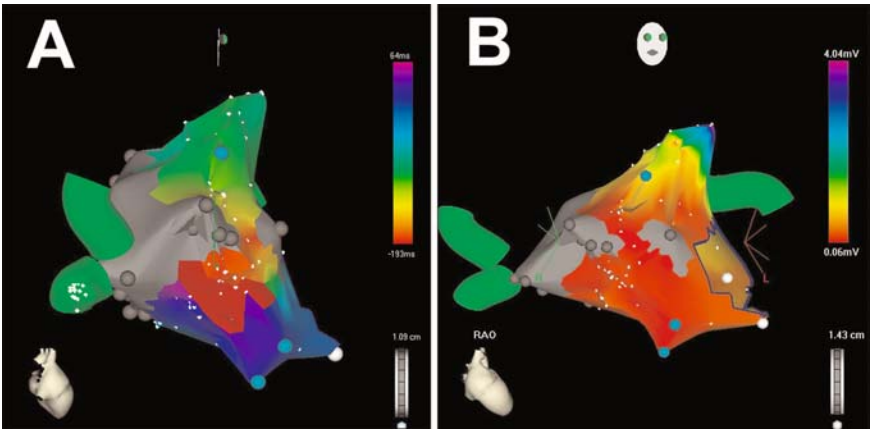

Fig. 4 A, B. Electroanatomic mapping of the left atrium during atrial tachycardia in the third presented case. **A** Right lateral view of the activation mapping with an 'early-meets-late' pattern in the upper left aspect of the atrial septum. **B** Bipolar voltage mapping is displayed in right anterior oblique view with evident low voltage (0.06 mV) around the incomplete line (*in grey*) from the medial mitral annulus to the right superior pulmonary vein. Of interest, the extension of scar tissue (*in grey*) after segmental pulmonary vein ablation. See text for further explanation

voltage of the critical area may be indicative of how difficult the ablation is expected to be. All these elements are essential to rationalise the approach to every single case, in order to plan a successful and safe ablation strategy. As a speculative aspect, this case addresses also the problems related to macroreentrant tachycardias around the peri-pulmonary lesions or involving a conduction gap of an incomplete linear lesion, which may occur even late after ablation in the left atrium for atrial fibrillation, possibly affecting the long-term benefit of the procedure. For atrial fibrillation ablation, a tailored approach for each patient, based on conventional and non-conventional data, should identify and target the arrhythmogenic substrate, thus avoiding overtreatment and its long-term electrical and, possibly, haemodynamic consequences.

The last case is a 21-year-old male patient with complex congenital heart disease, which included single ventricle, transposition of the great vessels, pulmonary valve stenosis, and persistence of the left superior vena cava. At the age of four, he underwent a Fontan operation with insertion of the left superior vena cava in the left pulmonary artery, of the right superior vena cava in the right pulmonary artery with direct closure of its orifice in the right atrium, which, in turn, was connected through a conduit to the pulmonary artery. In the same intervention, the tricuspid orifice was closed by a prosthetic patch, to separate venous from arterial blood flow. Six months before the procedure, the patient had episodes of what completely resembled a typical common atrial flutter on surface ECG, with 285-ms cycle length and 2:1 atrioventricular conduction ratio. In spite of therapy with amiodarone, the arrhythmia recurred and was responsible for syncope. Before the procedure, since the coronary sinus had not been visualised or cannulated in the past, a bipolar catheter was positioned in the oesophagus to stably record a left atrial electrogram, serving as reference. Afterwards, the right atrium was electroanatomically mapped with a long sheath to support the roving catheter on spontaneous rhythm at a cycle length of 920 ms, which was found to originate close to the os of the coronary sinus. On this rhythm, the chamber volume was 265 ml. The clinical arrhythmia was then reproducibly induced by programmed right atrial stimulation. After having set the window of interest as in the previous case, high density electroanatomic mapping was performed. As shown in Fig. 5A, activation in the right atrium covered the entire length of the flutter cycle with a mid-diastolically activated area located in the low lateral right atrium. From this area, the activation proceeded simultaneously anterior and posterior to the inferior vena cava and then started a single counter-clockwise loop, resembling the one of typical common atrial flutter. Interestingly, the pathway of diastolic activation had apparently no anatomic or acquired boundaries, and scar tissue was observed in a very limited area, not strictly in relation with the diastolic

pathway. Moreover, at the analysis of the bipolar voltage map on tachycardia (Fig. 5B), the diastolic pathway was clearly evident as a channel of very low voltage (0.05 mV), limited anteriorly and posteriorly by areas of preserved/normal voltage (0.5–5 mV). A plausible explanation of the presence of a re-entrant circuit without an anatomically protected isthmus could be as follows. At flutter cycle, functional conduction block occurred linearly in the transitional areas between low and preserved voltage, and these lines served as anterior and posterior boundaries to the diastolic pathway, thus allowing and stabilising re-entry. Of interest, the anterior right atrium, where the prosthetic patch was positioned on the tricuspid orifice, showed a relatively preserved voltage, suggesting a possible neogenesis of atrial tissue on the patch, positioned early during patient life. Entrainment mapping in the diastolic pathway was not possible due to lack of capture even at the maximum output. Radiofrequency energy (cool-tip catheter, maximum output 40 Watts) was delivered in the area identified as critical by electroanatomic mapping in order to transect completely, from posterior to anterior, the diastolic pathway. This resulted in termination of the tachycardia after prolonging the cycle length and producing a line of double potentials. Afterwards, the clinical flutter was no longer inducible even by very aggressive atrial stimulation. This induced a non-clinical atrial flutter with positive P wave in the inferior leads and a shorter cycle length (265 ms). High density electroanatomic mapping showed that right atrial activation was equal to the tachycardia cycle length, with a mid-diastolically activated area corresponding to the entire vertical length of the crista terminalis and a single loop re-entry rotating around the complete perimeter of the right atrium (Fig. 5C, D). Possibly, in this very enlarged atrial chamber, even transverse conduction over the crista terminalis may serve as slow conduction pathway of a re-entrant circuit in the right atrium. Since this arrhythmia was not clinical, the creation of a vertical and complete line of bidirectional block, was thought to be challenging and possibly proarrhythmic if incomplete, it was decided not to target this second arrhythmia morphology. On the same previously ineffective antiarrhythmic drug, the patient has been asymptomatic in the follow-up.

The experience acquired from this case also shows how electroanatomic mapping can provide all the necessary data for a tailored and evidence-based approach to ablation of complex re-entrant arrhythmias. Moreover, the information gathered can increase our knowledge on peculiar phenomena occurring in particular cases.

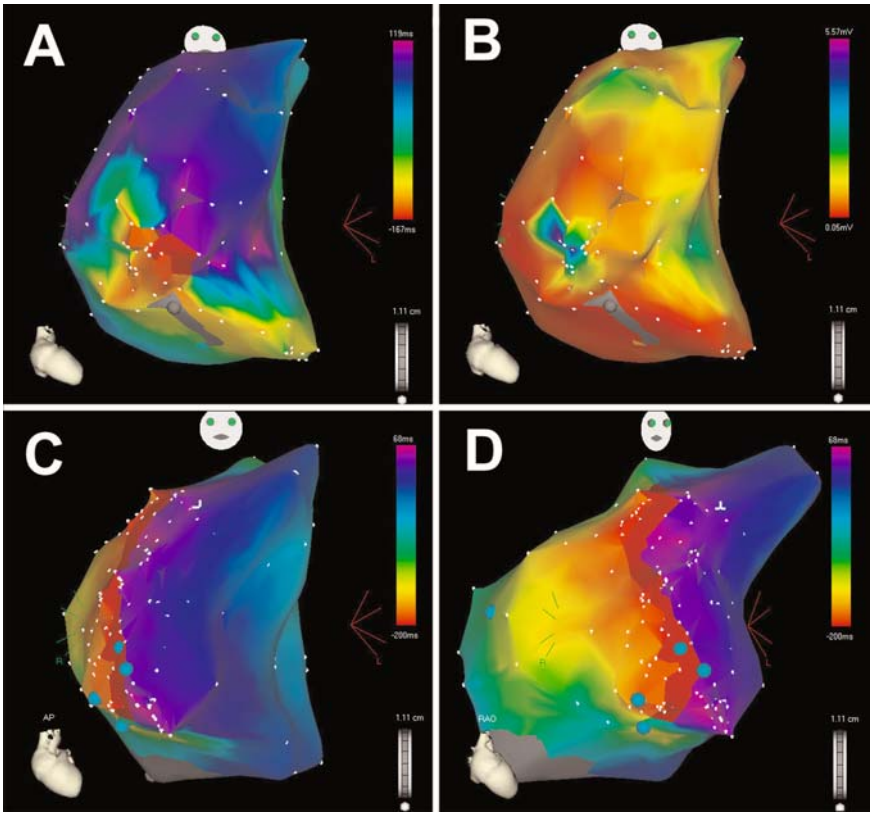

Fig. 5. Electroanatomic mapping of the right atrium during the clinical (**A, B**) and non-clinical (**C, D**) atrial flutter in the last presented case. **A, B** Caudal right anterior oblique view; **C, D** Antero-posterior and right anterior oblique projection, respectively. **A** Activation mapping with an 'early-meets-late' pattern and a diastolically activated isthmus in the lateral low right atrium, where the 'latest' activated area (*in purple*) encounters the 'earliest' activated area (*in red*). **B** Bipolar voltage mapping with a clear difference in voltage between the isthmus (0.05 mV) and the surrounding anterior and posterior areas (0.5–5 mV). **C, D** Activation mapping during the non-clinical atrial flutter, with a clear 'head-meets-tail' pattern in the crista terminalis, which in this morphology serves as slow pathway for re-entry. See text for further explanation

Summary and Future Perspectives

These samples of the experience gathered in our project support the hypothesis that electroanatomic mapping has an essential role in the approach to complex focal or re-entrant arrhythmias. In fact, a detailed analysis of the

arrhythmogenic substrate, other than being the core for a successful ablation strategy, may be a key issue in 'learning before burning' and it may anticipate when ablation could be particularly difficult and failure expected. Moreover, increased experience in electroanatomic mapping, together with technology improvements, such as imaging integration, should lead to the simplification of complex procedures, with an expected reduction in the procedure fluoroscopy time and an increased success rate. Whether this will expand the indication for ablation in complex cases remains to be demonstrated by further studies.

Appendix

The following is the list of the investigators participating in the Project of Electro-Anatomic mapping for Complex arrhythmia Evaluation (PEACE):

Roberto Verlato, Pietro Turrini, Unità di Elettrofisiologia Diagnostica ed Interventistica, Ospedale Civile di Camposampiero, Camposampiero (Padua); Raffaele Luise, Dipartimento di Cardiologia-Elettrofisiologia, Clinica Villa Pini d'Abruzzo, Chieti; Luigi Sciarra, Leonardo Coro', Unità Operativa di Cardiologia, Ospedale di Conegliano (Treviso); Emanuele Bertaglia, Francesca Zerbo, Dipartimento di Cardiologia, Ospedale Civile di Mirano (Venice); Antonio Fusco, Alfredo Vicentini, Laboratorio di Elettrofisiologia, C.C. dott.Pederzoli, Presidio Ospedaliero ULSS22-Regione Veneto, Peschiera del Garda (Verona); Maria Grazia Bongiorni, Giuseppe Arena, Unità di Aritmologia, Dipartimento Cardiotoracico, Azienda Ospedaliera Universitaria Pisana, Pisa; Nicola Bottoni, Fabio Quartieri, Unità Operativa di Cardiologia Interventistica, Dipartimento di Cardiologia, Azienda Ospedaliera S.Maria Nuova, Reggio Emilia; Gemma Pelargonio, Antonio Dello Russo, Laboratorio di Elettrofisiologia, Istituto di Cardiologia, Dipartimento di Medicina Cardiovascolare, Università Cattolica del Sacro Cuore, Rome; Fabrizio Drago, Massimo Silvetti, Dipartimento Medico-Chirurgico di Cardiologia Pediatrica, Ospedale Bambino Gesù, Rome; Andrea Avella, Francesco Laurenzi, Sezione Elettrofisiologia-Elettrostimolazione, II Unità Operativa di Cardiologia, Ospedale S.Camillo, Rome; Maurizio Del Greco, Massimiliano Marini, Laboratorio di Elettrofisiologia U.O. di Cardiologia, Ospedale S.Chiara, Trento; Raffaella Marazzi, Fabrizio Caravati, Laboratorio di Elettrofisiologia, Dipartimento di Scienze Cardiovascolari, Ospedale di Circolo e Fondazione Macchi-Università dell'Insubria, Varese.

References

1. Natale A, Newby KH, Pisanò E et al (2000) Prospective randomized comparison of antiarrhythmic therapy versus first-line radiofrequency ablation in patients with atrial flutter. J Am Coll Cardiol 35:1898–1904
2. Cheng CHF, Sanders GD, Hlatky MA et al (2000) Cost-effectiveness of radiofrequency ablation for supraventricular tachycardia. Ann Intern Med 133:864–876

3. Kalman JM, VanHare GF, Olgin JE et al (1996) Ablation of 'incisional' reentrant atrial tachycardia complicating surgery for congenital heart disease: use of entrainment to define a critical isthmus of conduction. Circulation 93:502–512
4. Baker BM, Lindsay BD, Bromberg BI et al (1996) Catheter ablation of clinical intraatrial reentrant tachycardias resulting from previous atrial surgery: localizing and transecting the critical isthmus. J Am Coll Cardiol 28:411–417
5. Triedman JK, Bergau DM, Saul JP et al (1997) Efficacy of radiofrequency ablation for control of intraarial reentrant tachycardia in patients with congenital heart disease. J Am Coll Cardiol 30:1032–1038
6. Della Bella P, Fraticelli A, Tondo C et al (2002) Atypical atrial flutter: clinical features, electrophysiological characteristics and response to radiofrequency catheter ablation. Europace 4:241–253
7. Jaïs P, Shah DC, Haïssaguerre M et al (2000) Mapping and ablation of left atrial flutters. Circulation 101:2928–2934
8. Shah D, Jaïs P, Haïssaguerre M (2002) Electrophysiologic evaluation and ablation of atypical right atrial flutter. Card Electrophysiol Rev 6:365–370
9. Ouyang F, Ernst S, Vogtmann T et al (2002) Characterization of reentrant circuits in left atrial macroreentrant tachycardia: critical isthmus block can prevent atrial tachycardia recurrence. Circulation 105:1934–1942
10. Heist EK, Doshi SK, Singh JP et al (2004) Catheter ablation of atrial flutter after orthotopic heart transplantation. J Cardiovasc Electrophysiol 15:1366–1370
11. Nabar A, Timmermans C, Medeiros A et al (2005) Radiofrequency ablation of atrial arrhythmias after previous open-heart surgery. Europace 7:40–49
12. Lukac P, Pedersen AK, Mortensen PT et al (2005) Ablation of atrial tachycardia after surgery for congenital and acquired heart disease using an electroanatomic mapping system: which circuit to expect in which substrate? Heart Rhythm 2:64–72
13. Ott P, Kelly PA, Mann DE et al (1995) Tachycardia-induced cardiomyopathy in a cardiac transplant recipient: treatment with radiofrequency catheter ablation. J Cardiovasc Electrophysiol 6:391–395
14. De Ponti R, Zardini M, Tritto M et al (1999) Sistema non fluoroscopico per mappaggio cardiaco elettroanatomico tridimensionale (CARTO). Cardiologia: 44 (Suppl I):387–390
15. Leonelli FM, Tomassoni G, Richey M et al (2001) Ablation of incisional atrial tachycardias using a three-dimensional nonfluoroscopic mapping system. Pacing Clin Electrophysiol 24:1653–1659
16. Markowitz SM, Brodman RF, Stein KM et al (2002) Lesional tachycardias related to mitral valve surgery. J Am Coll Cardiol 39:1973–1983
17. Magnin-Poull I, De Chillou C, Miljoen H et al (2005) Mechanism of right atrial tachycardia occuring late after surgical closure of atrial septal defects. J Cardiovasc Electrophysiol 16:681-687
18. Gerstenfeld EP, Callans DJ, Dixit S et al (2004) Mechanisms of organized left atrial tachycardias occuring after pulmonary vein isolation. Circulation 110:1351–1357
19. Kobza R, Hindricks G, Tanner H et al (2004) Late recurrent arrhythmias after ablation of atrial fibrillation: incidence, mechanisms, and treatment. Heart Rhythm 1:676–683
20. Cummings JE, Schweikert R, Saliba W et al (2005) Left atrial flutter following pulmonary vein antrum isolation with radiofrequency energy: linear lesions or repeated isolation. J Cardiovasc Electrophysiol 16:293–297
21. Kilicaslan F, Verma A, Yamaji H et al (2005) The need for atrial flutter ablation fol-

lowing pulmonary vein antrum isolation in patients with and without previous cardiac surgery. J Am Coll Cardiol 45:690–696
22. De Ponti R, Avella A, Bertaglia E et al (2004) Standardized setting of the window of interest in the electroanatomic mapping of reentrant tachycardias to identify the critical area: a multicentric Italian evaluation. Eur Hear J 25:280 (abs)